Sub-Surface LIPSS Induced by Single Femtosecond Laser Pulses

Pierre Lorenz*, Andriy Lotnyk, Martin Ehrhardt, and Klaus Zimmer

Leibniz Institute of Surface Engineering (IOM), Permoserstr. 15, 04318 Leipzig, Germany

Corresponding author's e-mail: pierre.lorenz@iom-leipzig.de

The generation of periodic surface structures (LIPSS) using Laser is a well-known and extensively researched effect. The majority of known und studied LIPSS are generated by multi-pulse irradiation, with single-pulse LIPSS being currently under-researched. This study investigated the single-pulse generation of LIPSS on a silicon Si(100) surface covered with a SiO_2 layer. The layer system was irradiated by single IR fs laser pulse (260 fs, 1030 nm, 2µJ). Single pulse irradiation allows the production of LIPSS on the Si surface below the SiO_2 layer without disturbing the SiO_2 layer. These subsurface LIPSS have a period of approximately 1 µm. In addition, multiple, laterally separated single pulses were applied to the SiO_2/Si and the effect of the formed structures as a function of the spacing and geometry of the single pulses was systematically analyzed. When employing multiple single pulses, it is evident that when the distance between irradiation points is below 20 µm, LIPSS areas are formed that are significantly larger than the area of the separated single points especially in polarization direction.

DOI: 10.2961/ilmn.2025.03.2006

Keywords: LIPSS, silicon, fs-laser, single pulse, sub-surface damage

1. Introduction

Laser-induced periodic surface structures (LIPSS) on silicon using ultrashort laser pulses have garnered significant attention in the scientific community[1-6]. LIPSS are self-organized nanoscale surface patterns that form when a material is irradiated with intense laser pulses [7-9]. They were first discovered by Birnbaum in 1965[10] and have since been studied in detail on a variety of materials (metals, polymers, semiconductors and dielectrics)[11]. Two different kind of LIPSS was detected: low spatial frequency LIPSS (LSFL) and high spatial frequency LIPSS (HSFL)[9]. The periodicity of the LSFL is nearby the applied Laser wavelength and the periodicity of the HSFL is distinct lower than the applied Laser wavelength.

The theoretical description of the LIPSS has been studied very intensively and is still the subject of current research[12]. The formation of LSFL is typically attributed to the interaction of strongly polarized laser light with scattered light originating from the surface roughness of the substrate. Consequently, the excitation of surface plasmon polaritons (SPP) is a widely employed explanatory model[13, 14]. The laser treatment of silicone was intensively studied[5, 15, 16] where the LIPSS formation is found for multi pulse treatment. The experimental result presented that a single pulse irradiation of a crystalline Silicon result in the formation of an amorphous layer[15]. Furthermore, the LIPSS process was also studied on layer systems [17-19]. Liao et al.[19] and Nürnberger et al. [17] reported the formation of sub-surface LIPSS on a silicon surface below a SiO_2 layer using multiple 532 nm laser pulses. Furthermore Florian et al. [18] reported the formation of sub-surface LIPSS on a CrN surface covered with an oxide layer where a coexistence of HSFL on the oxide layer surface and LSFL on the CrN / oxide layer interface was found.

Most of the investigated LIPSS on pure silicon and on silicon underneath an oxide layer have been formed by multi-pulse irradiation. However, there are studies that have shown that single femtosecond pulses allow the formation of LIPSS under special confinement conditions[20].

The focus and novelty of the work carried out is the investigation of the generation of sub-surface LIPSS on a silicon surface below an oxide layer by means of a single pulse.

Furthermore, the work of Liu et al. [15] presented that the already the single pulse treatment of a pure silicon surface result in the formation of an amorphous layer as well as in the formation of a zone with dislocations. It can be assumed that these defect layers have an influence on the interaction with the laser radiation and thus on the formation of LIPSS. This was investigated as a second aspect in this work in which single pulses were geometrically superimposed while systematically changing the distance between the pulses and the geometry (orientation of the single pulses to each other). This selective overlap can be used to investigate the influence of laser-induced modifications on LIPSS formation. Unlike the common approaches[21-24], which use a high number of laser pulses or high pulse overlap, our approach uses single pulses with small pulse overlap to systematically investigate the influence of pre-modifications on LIPSS formation.

2. Experimental Details

A crystalline silicon wafer Si (100) (from Si-Mat – Silicon Materials e.K, prime grade) covered by a 109 nm silicon di oxide SiO_2 layer induced by thermal oxidation was irradiated by femtosecond single laser pulses. Therefore, a Gaussian laser beam, using a PHAROS PH2-20 W from Light Conversion, with a wavelength of λ = 1030 nm, a pulse duration of Δt_p = 260 fs and a M^2 = 1.2 was focused by a f-theta lens with a focal length of the f_{opt} = 163 mm on the sample surface. The focused laser beam exhibit a Gaussian radius of ω_0 = (23 ± 2) µm determined by Liu plot [25]. The laser pulse exhibits a pulse energy of E_p = 2 µJ. The position of the laser pulse on the sample was change by a galvo scanner. The time between the single pulses was set to 1s. Single pulses with different spacings and geome-

tries (defined geometries as well as random distributed dots) were applied to the wafer surface. A summary of the applied spot geometries is show in Fig. 1 where the distance was variated from 5 µm up to 20 µm. Beside the determined geometries also random distributed laser spots was applied.

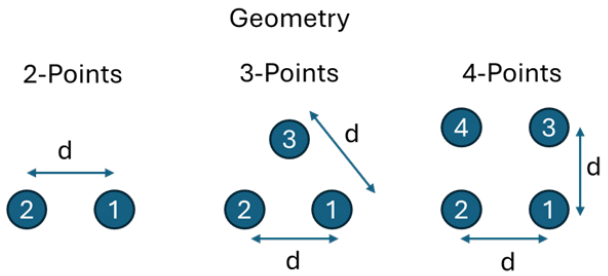

Fig. 1 Summary of the Laser spot geometry. (1: first pulse, 2: second pulse, 3 third pulse, 4: fourth pulse).

The absorption coefficient of the SiO_2 layer is with $\alpha = 1.6336$ cm^{-1} [12] distinct smaller than the absorption coefficient of silicone $\alpha = 29.168$ cm^{-1} [26] at room temperature. The laser irradiated surfaces was measured by optical microscopy (OM), scanning electron microscopy (SEM – Zeiss Gemini Ultra 55) and atomic force microscopy (AFM -Bruker Dimension ICON). The microstructure of sub-surface LIPSS was studied by transmission electron microscopy (TEM). Cross-sectional thin film specimens were prepared by focused ion beam (FIB). High-resolution TEM measurements were performed using a probe Cs-corrected FEI Titan3 G2 60-300 operated at 300 kV accelerating voltage. The images were recorded using a Gatan US1000XP P CCD camera. Energy dispersive X-Ray spectroscopy (EDX) was performed in scanning TEM mode. The EDX maps were acquired with Super-X detector using Bruker Esprit software.

3. Experimental Results

The SiO_2 / Si surface was irradiated with infrared single laser pulses with a pulse energy of 2 µJ with different geometries and distances. An overview is summarized in Fig. 2. The microscopic and scanning electron image of 2 dots, 3 dots (equilateral triangle) and 4 dots geometry (square), geometry overview is summarized in Fig. 1, with a dots distance from 5 µm up to 15 µm is shown in Fig. 2. The single pulse irradiation of the 109 nm SiO_2 layer / Si(100) system result in a bulge. Based on the SEM images with an average diameter of (9.8 ± 0.3) µm (see Fig. 4). In fig. 3, an exemplary optical image in comparison to a AFM measurement (cross section through the center of the bulge) is presented. The AFM measurements presented that the bulge presented an average height of (285 ± 5) nm at a diameter of (8.6 ± 0.5) µm. The optical image shows a bright color gradient in the center of the bulge. This can most likely be explained by the fact that the SiO_2 layer stands out from the Si wafer in the center of the irradiation. The optical visible color effects are then a result of interference effects at the additional interface. Surprisingly, OM image shows further structures outside the bulge.

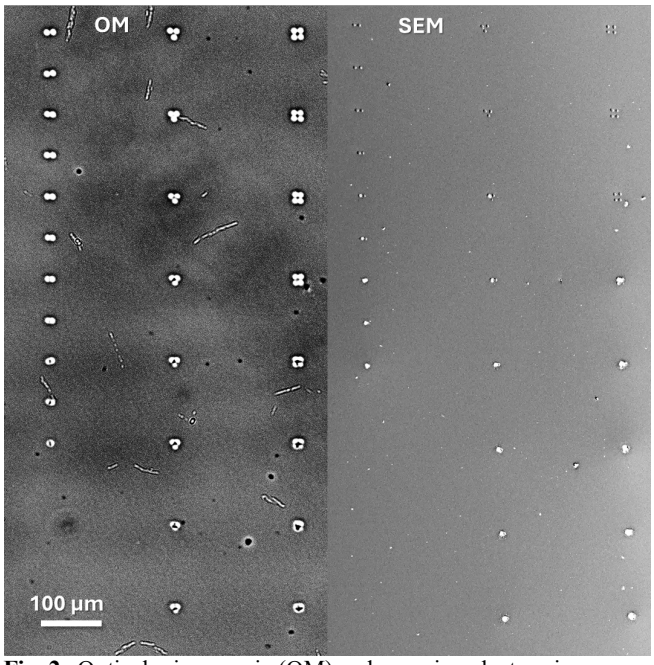

Fig. 2 Optical microscopic (OM) and scanning electron image (SEM) of laser irradiated SiO_2/Si surface with different geoemtriey and pulse distance from d = 15 µm to 5 µm.

A ring with periodic structures with a period of around 1 µm is visible around 4-6 µm from the center of the irradiation and elevation, respectively. The AFM image presented an almost flat and smooth surface in the optical detected ring area, the surface roughness in the ring area is comparable to the non-irradiated region.

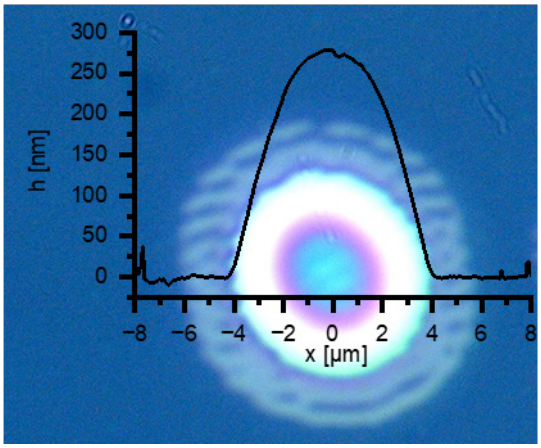

Fig. 3 Exemplary optical image of a single laser spot irradiated SiO_2 layer/Si System in comparison to the height profile measured by AFM.

That means the single laser pulse induced periodic surface structure is located at the SiO_2/Si interface. The laser fluence in the center of the gaussian laser beam can be calculated by:

$$\Phi(r=0) = \frac{2 \cdot E_p}{\pi \cdot \omega_0^2} = (240 \pm 20)\ \frac{mJ}{cm^2}. \qquad (1)$$

In the ring area r = 4 -6 µm the laser fluence can be estimated by:

$$\Phi(r = 4\,\mu m \ \dots\ 6\,\mu m) = \Phi(r = 0) \cdot e^{-\frac{r^2}{2\omega_0^2}} = (237 \pm 20)\frac{mJ}{cm^2} \dots (233 \pm 20)\frac{mJ}{cm^2}. \quad (2)$$

That means the LIPSS structures appear at laser fluence between 233 mJ/cm² and 237 mJ/cm² where the total accuracy of the laser fluence is in the range of ~10%. In the next step randomly, distributed dots were performed. A typical result is shown in Fig. 4. If the dots come closer together or overlap, the SiO_2 layer becomes detached and the periodic ring structure on the surface of the SiO_2 layer becomes recognizable. Furthermore, a round depression with an average diameter of (6.57 ± 0.18) µm is visible in the center of the irradiation. This depression can be assigned to the evaporation of the Si during single pulse irradiation.

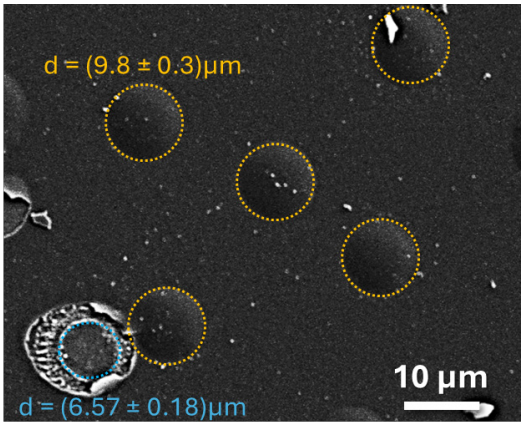

Fig. 4 SEM image of randomly distributed single laser induced dots.

Based on Eq. 2 a single pulse evaporation threshold of confined silicon under a 109 nm SiO_2 layer is Φ_{th}^{eva} = (238 ± 20) mJ/cm². Especially the random distribution experiment presented that the resulting surface structures are directly dependent on the distance of the laser inducer dots. Therefore, the distance as well the geometry of the laser induced dots was systematically studied.

3.1 2 Point geometry

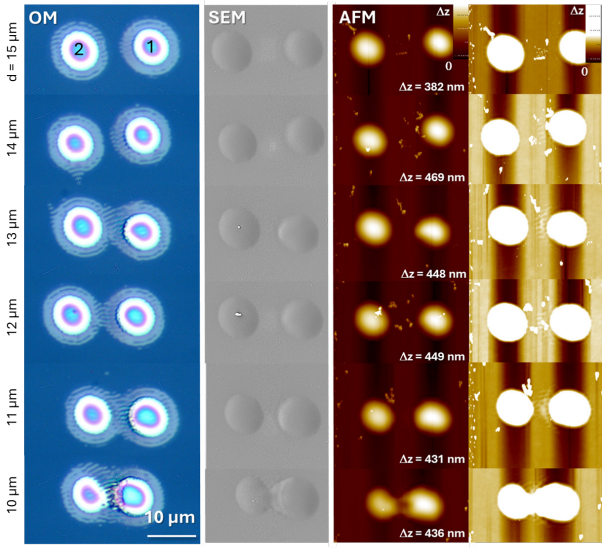

Fig. 5 OM, SEM and AFM images of single pulse laser irradiated 2-point dots with different distances.

In Fig. 5 OM, SEM as well as AFM images of a single laser pulse irradiated SiO_2/Si system with a 2-Point geometry (see Fig. 1) with different point distances from 10 µm to 15 µm are summarized. For distances above 13 µm the 2 dots exhibit the same shape like the separated single pulse dot presented in Fig. 3. At distances of 11 µm to 13 µm, the approach leads to the formation of additional LIPSS structures between the two points. This is very clearly recognizable in the optical image. In contrast to the separated single pulse dots, the formation of the LIPSS between the two points leads to a modification of the SiO_2 surface and LIPSS structures can be recognized on the SiO_2 surface using AFM. Furthermore, a very weak periodic modulation of the SiO_2 surface between the points can also be recognized at 14 µm. At d = 10 µm, the overlap of the two irradiated points leads to a bulging of the SiO_2 surface between the points. In the optical image, the connected LIPSS between the points are clearly visible, whereas in the AFM they can only be detected outside the bulge due to the additional bulging of the SiO_2. The recognized LIPSS on the SiO_2 surface exhibit a periodicity of p = (950 ± 90) nm and an average P-V value of Δz = (6.4 ± 1.6) nm where individual periodic structures exhibit a P-V of up to 12 nm. A typical cross section of a LIPSS structure at a distance of d = 13 µm is show in Fig. 6. The results suggest that the LIPSS nearby the center, see center line Fig. 6, exhibit a larger p-V value. Furthermore, the analyzing of the AFM data presented no dependency of the periodicity and P-V Value from the distance d (at d = 11 – 13 µm).

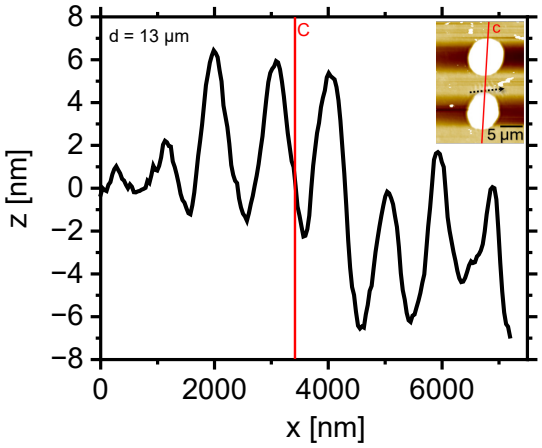

Fig. 6 Exemplary cross section of the LIPSS structures on the SiO_2 surface taken between the two single spot at a distance of d = 13 µm (The black dashed line in the AFM image (top right) represents the position of the cross-section (black line) presented, and the red line marked with "C" marks the center line through the middle of each laser spot.).

The OM images presented at d = 11 – 13 µm the LIPSS structure are almost homogeneous distributed between the two dots where the AFM measurement presented that the LIPSS on the SiO_2 surface are localized nearby the first single laser pulse.

3.2 3 Point geometry

In agreement with the two-point geometry also the 3-point geometry was analyzed. A summary of the experimental results is shown in Fig. 7. At large spot distances of

d > 14 µm the typical result for separated single pulse spot can be found. At a distance of 13 - 14 µm, the irradiation again leads to an enlargement of the LIPSS area, especially in the center of the equatorial triangle which the three laser points create. Furthermore, in agreement with 2-point arrangement the overlap result in the formation of LIPSS on the SiO_2 surface. At d =15 µm, the SiO_2 surface LIPSS was detected nearby the first laser pulse in agreement with the results of the two-point arrangement. At smaller distances d = 10 - 12 µm, the overlap results in a partial cracking of the SiO_2 layer where the delaminated SiO_2 layer is mainly localized nearby the first laser pulse. The result suggests that the size if the delaminated area increased at decreasing distance d. At the delaminated area the SEM images presented the formation of rough LIPSS structures on the Si surface (see Fig. 8).

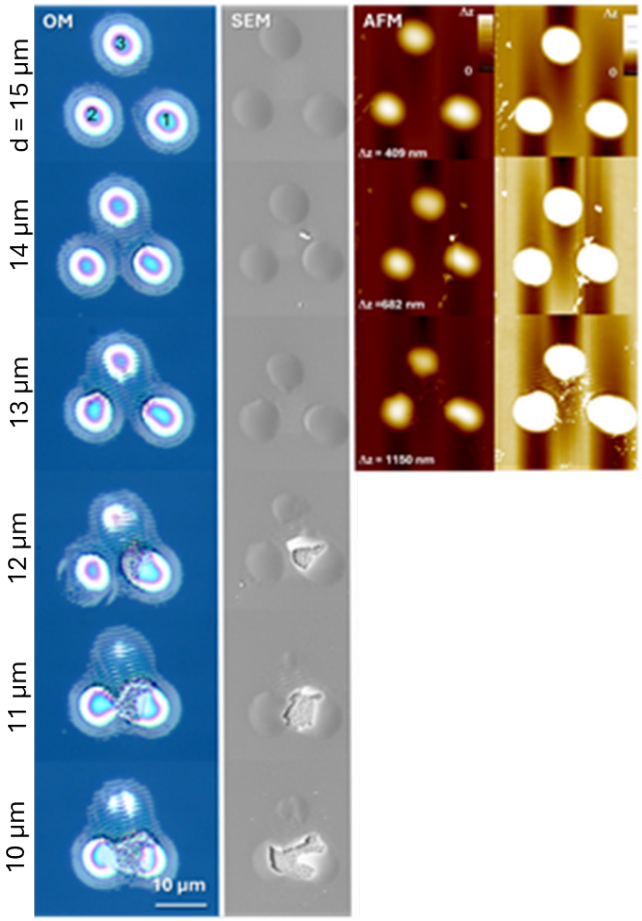

Fig. 7 OM, SEM and AFM images of single pulse laser irradiated 3-point dots with different distances.

The SEM image shows that no LIPSS are visible in the center of the laser spot and that rough periodic structures form around the laser spot. A periodicity of the LIPSS on the Si surface of (930 ± 60) nm can be detected. However, due to the roughness of the surface, the effects are only faintly visible. Furthermore the 3-point agreement at lower distances result in the partial periodic cracking of the SiO_2 (see Fig. 8).

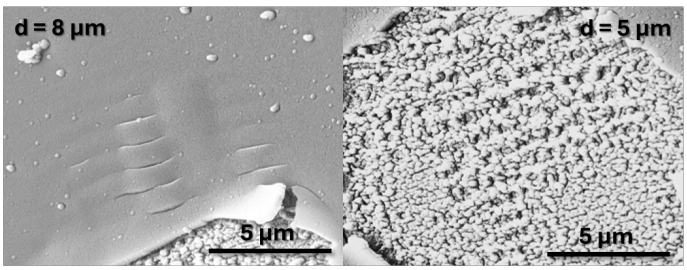

Fig. 8 (left) Exemplary SEM image of periodic cracked SiO_2 layer (3-point arrangement d = 8 µm) (right) Exemplary SEM image of Si surface after delamination of SiO_2 layer (3-point arrangement d = 5 µm).

3.3 4 Point geometry

Beside the 2- and 3- point arrangement also the 4-point arrangement was studied (summary see Fig. 9).

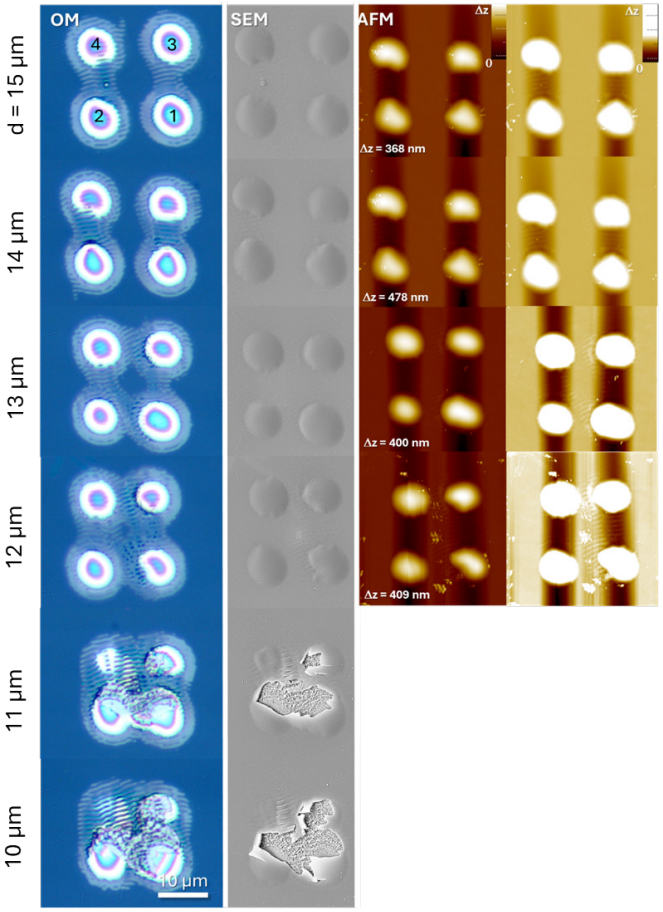

Fig. 9 OM, SEM and AFM images of single pulse laser irradiated 4-point dots with different distances.

Similar effect than already detected at the 2- and 3- point arrangement can be found. At large distances d > 15 µm the typical structures than separated single pulse dots can be found (see fig. 10). At d = 14 - 15 µm, the pulse overlap result in an increasing of the LIPSS area especially perpendicular to the LIPSS orientation (see Fig. 10). In agreement with the further measurement also LIPSS structures on the front side of the SiO_2 layer can be found by AFM.

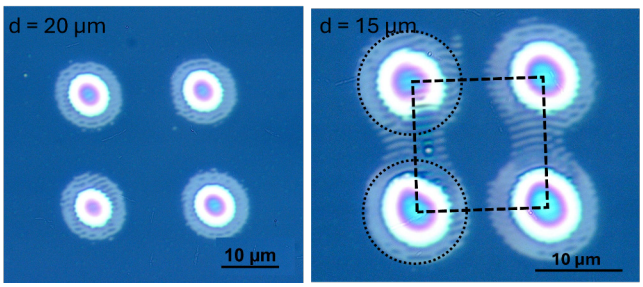

Fig. 10 Microscopic image of laser treated SiO_2/Si with 4 points at a distance of d = 20 µm (left) and d = 15 µm (right) (black dash circle: represented the original size of the LIPSS area at d = 20 µm; black dash square: represented the position of the center of the laser spots).

At d = 12 – 13 µm, in the optical image a joining of the LIPSS in both directions can be found in combination with LIPSS on the SiO_2 surface detected by AFM.
At d ≤ 11 µm the overlap result in the partial delamination of the SiO_2 layer. Furthermore, in agreement with the three-point arrangement also the 4-point result in the partial periodic cracking of the SiO_2 layer.

3.4 Microstructural studies

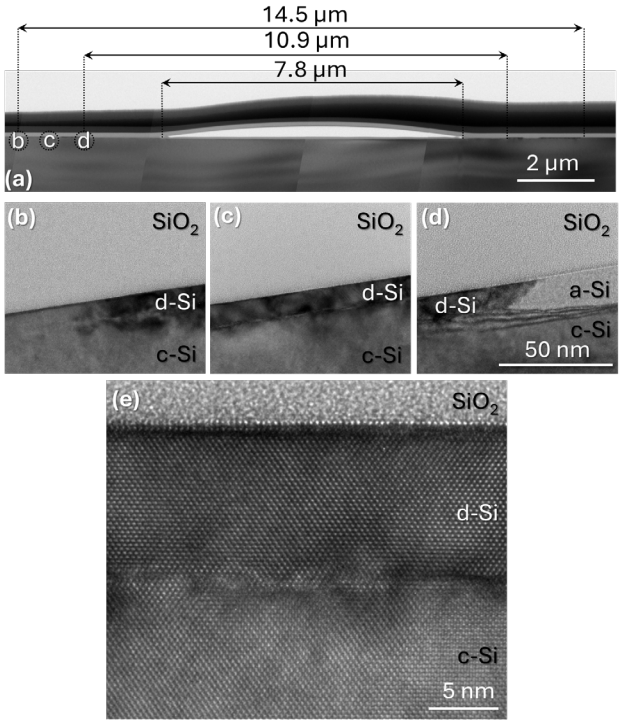

Fig. 11 Microstructure of a single dot of SiO_2/Si. (a) Bright-field TEMimage showing different zone after irradiation, (b)-(d) Bright-field TEMmicrographs from the corresponding areas marked in (a) and (e) High-resolution TEM image at position c.

Exemplary TEM images of a single dot of SiO_2/Si is shown in Fig. 11. FIB lamella was cut parallel to the LIPSS. Due to the lateral large length of the lamella the TEM measurements were performed in steps and the different images were assembled in a subsequent stage using an image editing program, result see in Fig. 11 (a). TEM measurements showed that the single pulse irradiation results in a center of the irradiation of a peeling off the SiO_2 layer up to a distance of 3.9 µm from the center as well as in the formation of an amorphous silicon layer (a-Si) on top of the crystalline silicon (c-Si). That means, a minimum laser fluence of (237 ± 20) mJ/cm² is necessary to induce a delamination of the SiO_2 layer, based on Eq. 1 and 2. The amorphous Si appears slightly lighter than the c-Si. The amorphous layer is formed up to a distance from ~ 5.45 µm from the center of the irradiation (see Fig. 11 (d)). The distance of ~ 5.45 µm means a laser fluence threshold of (233 ± 20) mJ/cm² based on Eq. 1 and 2. At a distance from ~5.45 µm up to 7.25 µm, recrystallize silicon (d-Si) was found partially separated from a-Si part (see fig. 11 (c)). Based on Eq. 1 and 2 a laser fluence range from about 228 to 233 mJ/cm² where the total accuracy of the laser fluence is in the range of ~10%. At higher distances no surface or sub surface modification was detected (see Fig. 11 (a)). Fig. 11 (e) presented a high-resolution TEM image at position c, marked in Fig. 11 (a). The images presented a clear separation between native c-Si and the recrystallize layer (d-Si) where the d-Si layer have a thickness of about 10 nm. The different effects can be summarized as a function of the laser fluence and the distance from the center of irradiation, see Table 1.

Table 1 Summary of the different detected effects depending on the calculated laser fluence and the distance from the center of the irradiation based on the analyzing of the TEM images as well as of the SEM, AFM and optical microscopic images.

Method	effect	laser fluence	Distance from center
TEM	SiO_2 delamination	> 237 mJ/cm²	≤ 3.9 µm
	Amorphous Si	233 – 237 mJ/cm²	5.45 µm
	Recrystallized Si	228 – 233 mJ/cm²	7.25 µm
	No effect	< 228 mJ/cm²	> 7.25 µm
SEM & AFM	Bulge formation on the SiO_2 surface		4.3 – 4.9 µm
OM	SiO_2 delamination	> 237 mJ/cm²	≤ 4 µm
	LIPSS formation	233 – 237 mJ/cm²	4 - 6 µm

Furthermore, a 4-point geometry was analyzed with a point distance of 15 µm. FIB lamella was prepared from point 2 to 4 (see fig. 1) perpendicular to the LIPSS orientation. The assembled TEM image is shown in Fig. 12 (a). In agreement to the single dot irradiation, shown in Fig. 11, the irradiation resulted in the center of the irradiation to a delamination of the SiO_2 layer and the formation of a bubble. Further a formation of region with amorphous and recrystallized silicon was found localized on the silicon surface. Furthermore, especially between the two irradiation points LIPSS structures were found, see Fig. 12. The periodic structure is separated in two regions: region α und region β, see Fig. 12 (b). The region α exhibit lateral width of ~ 650 nm. In this region a formation of an amorphous silicon was detected as well as a delamination of the SiO_2 lay-

er and a formation of a bubble, respectively. The bubble exhibits a height of ~ 50 nm and a width of ~140 nm. The TEM image represents a 2-dimensional section vertically through the LIPSS structures which means that the irradiation leads to a channel which is shown as a bubble in the section. In the vicinity of the bubble, amorphous Si is formed. In the region β there is a surface localized change in the silicon which appears darker in the TEM image and exhibit a lateral width of ~ 350 nm. This can be attributed to recrystallized silicon. It can be assumed that this area has an increased defect density. The period of the LIPSS structures results from the lateral width of region a and b and is ~ 1000 µm. Furthermore, the composition was analyzed by EDX, see Fig. 12 d-e. The EDX composition shows a clear separation between the SiO_2 layer and the Si after laser irradiation. Furthermore, the formation of an oxide layer was detected on the underside of the bubble.

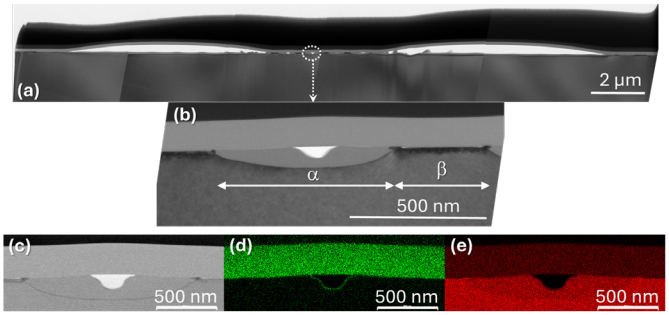

Fig. 12 (a)-(b) Bright-field TEM images of overlapping single laser pulses (at a 4 point geometry) with a distance of 15 µm. (c) Annular-bright field STEM image and (d)-(e) corresponding EDX maps of O and Si.

4. Discussion

The irradiation of SiO_2 layer / Si systems result in two different main effects the formation of a bulge in the center of the irradiation with a gaussian infrared femtosecond laser beam and the formation of sub-surface LIPSS localized in a ring-like area outside the formed bulge. This process is accompanied by the local amorphization of the silicon surface and the formation of a recrystallized Si surface at higher and lower laser fluences, respectively.

- Single pulse sub-surface LIPSS

The single pulse irradiation with an Infrared femtosecond laser pulse of a 109 nm SiO_2 / Si(100) system allows the fabrication of subsurface LIPSS at the Si surface at an estimated laser fluence of 233 – 237 mJ/cm^2 and to a surface near modification of the silicon: amorphization at 233-237 mJ/cm² and recrystallisation at 228-233 mJ/cm². The irradiation result in a modification of the silicon up to a distance from 7.25 µm from the center of the irradiation which implies an modification threshold of 228 mJ/ cm². Already P. Nürnberger analysed the LIPSS formation on SiO_2/Si with multi-pulse irradiation using 532 nm ns-laser pulses [27] Reference experiments on pure silicon, directly before the laser treatment the natural oxygen layer was removed by HF, presented no formation of LIPSS induced by a single laser pulse (For reasons of clarity, the findings are not shown in the results.). The sub-surface LIPSS are perpendicular to the linear polarization of the laser beam and the formed LIPSS periodicity with ~ 1000 nm is nearby the laser wavelength used. That means the formed LIPSS can be characterized as Type I low spatial frequency laser induced periodic surface structures (Type LSFL-I) [9]. The origin of these LIPSS can be correlated to the formation of a surface plasmon polariton (SPP)[12]and additional interference effects. The possibility of forming an SPP is primarily dependent on the properties of the interface. For excitation of SPP at a particular interface, the condition in Eq. 3 has to be fulfilled [28].

$$\varepsilon_1' * \varepsilon_2' + \varepsilon_1'' * \varepsilon_2'' < 0, \quad (3)$$

where $\varepsilon_1 = \varepsilon_1' + i\varepsilon_1''$ is the dielectric function of the substrate and $\varepsilon_2 = \varepsilon_2' + i\varepsilon_2''$ is the dielectric function of the medium in contact with the substrate surface. The melting temperature of Si is 1683 K and the evaporation temperature 3533 K and of SiO_2 of 1983 K and >2473 K, respectively.

Table 2 Summary of the dielectric function.

	ε′	ε′′
Air	1	0
SiO_2 (300 K)	2.16	0
SiO_2 (1600 K)	-7.08	2.84
SiO_2 (2300 K)	-11.8	4.44
Si	11.7	0

At room temperature, the condition for the formation of a SPP is not fulfilled (see Tab 3).

Table 3 Summarized of calculation of Eq. 3 at the different interfaces.

T = 300 K	$\varepsilon_1' * \varepsilon_2' + \varepsilon_1'' * \varepsilon_2''$
Air/SiO_2	2.16 >0
SiO_2/SI	25.272 > 0
Air/Si	11.7>0

However, the absorption of the laser beam, mainly by the silicon, result in an increasing electron density among other things by the increasing of the temperature, first of the electron temperature if we assumed a two temperature model [29]. The laser irradiation induced increasing of the electron density result in a decreasing of the real part and an increasing of the imaginary part of the dielectric function of the Si and the SiO_2[30]. The estimation of the dielectric function[30] suggests that the formation of an SPP is possible at increased electron densities. The increasing of the electron density by femtosecond laser radiation was theoretical described by Liu et al.[15]. For example, assuming a

charge density of ~ $2*10^{22}$ cm^{-3}, the condition for an SPP would be fulfilled. That means, as a result of the laser irradiation, the silicon is excited and can take on metallic properties. It can be assumed that SPP is formed between the air and the excited silicon in thin SiO_2 layers. The formation of SPP between SiO_2 and the excited Si is also possible[27]. Single pulse irradiation studies were also carried out on thicker SiO_2 layers (~ 1 µm) and no LIPSS formation could be detected (in order not to disturb the clarity of the paper, the data were not presented in the results section. This can be suggested that the formation of the SPP between the excited silicon and the air is the dominant process. However, the formation of a SPP does not explain the effect that a single pulse irradiation of a pure silicon does not present LIPSS formation. The estimation presented that the formation of SPP is possible from the electromagnetic point of view. However, for the formation of a SPP an initial scattering is necessary. In the classical point of view the scattering is performed on an initially rough surface. For the subsurface LIPSS Various scattering processes are conceivable: Scattering at the SiO_2 surface, scattering at inhomogeneity in the SiO_2 layer and scattering at the SiO_2/Si interface. Furthermore, interference effect due to the SiO_2 layer cannot be excluded. This interference effect may explain the need for the SiO_2 layer. In conclusion, the cause of LIPSS formation cannot be proven beyond doubt. Further investigations of the sub-surface LIPSS formation are necessary as a function of the confinement layer (thickness, optical properties and defect density). The single pule laser pulse induced LIPSS formation under confinement was already find on other systems[20]. Furthermore, the TEM analysis presented sub-surface modification in the silicon beside the periodic surface topography. The periodic alternation of region a (amorphous silicon) and region b (recrystallized silicon) measured in TEM images leads to the conclusion that there is a periodic variation of the laser fluence close to the surface during irradiation (region a: higher fluence, region b: lower fluence). Assuming the results of the single pulse experiment, it can be roughly estimated that the effective laser fluence in region a is 233 - 237 mJ/cm^2 and in region b is 228 -233 mJ/cm^2. This near-surface variation of the laser fluence suggests the formation of an SPP at the SiO_2/Si interface. At this stage, it should be noted that interference effects on the formation of the LIPSS structures cannot be ruled out, based on the results that have been obtained thus far. Based on the current data situation, the SPP hypothesis represents a possible explanation of the effect. However, further experiments must be carried out to fully clarify the phenomenon.

- Bulge formation

The laser irradiation of the SiO_2/Si system result in the formation of the bulge in the centre of the irradiation. The laser beam is mainly absorbed by die Silicon substrate and in the centre of the laser beam the irradiation result in an evaporation of the silicon. The SEM images presented a smooth crater on the Si surface after removal the SiO_2 (see Fig. 4). The laser-induced irradiation effect induced a deformation of the SiO_2 layer which finally result in the detected bulge structure. A similar experiment was already reported by Rapp et al.[31], the femtosecond irradiation of a SiO_2 / Si system with femtosecond laser pulses result in a micro explosion and a modification of the Si was found.

- Pulse distance variation

Already a single pulse allows the fabrication of LIPSS structures. However the approach of single pulse allows the fabrication of LIPSS structures between the laser dots. This approaching concept was studied with different geometries: 2 point, 3-point as well as 4-point (see Fig. 1). At 2-point geometry, for point distances $d \geq 15$ µm both dots show the typical size of single point irradiation. However, at $d < 15$ µm an influence of the first dot on the second dot can be found. The TEM measurement presented, that the first pulse induced an amorphization and recrystallization with defects was produced where the modifications can be found up to a distance of 7.25 µm from the distance from the center of irradiation. That means the single pulse detected lateral modification layer agree very well with the point distance geometry of 15 µm. Similar single pulse modification on pure silicon was already reported by Liu et al.[15]. Liu et al.[15] reported, at a gaussian radius of 5.5 µm, 150 mJ/cm^2 is suitable to induced a single pulse amorphization of pure silicon. Furthermore, a melting threshold of 130 mJ/cm^2 was estimated. This value is a little bit smaller than the found modification threshold of 228 mJ/cm^2 for the SiO_2/Si. The first pulse causes melting and most likely partially vaporization of the silicon at the centre of the irradiation to form a bulge in the SiO_2 layer. Outside the bulge an area of LIPSS is formed on the SiO_2/Si interface. Furthermore, a modification area based on amorphous Si and Si with recrystallized silicon is formed around the irradiation (see Fig. 11). If a second laser pulse is added at large spot distances d, no interaction can be detected. However, if the distance is smaller or equal than 15 µm, the second laser pulse interacts with the modification layer. This results in an increase in the LIPSS area. The magnification is mainly perpendicular to the LIPSS, i.e. parallel to the direction of polarization. This is particularly visible in the 4-point geometry, see Figures 9 and 10. Furthermore, the overlapping of two pulses results in the formation of a periodic structuring of the SiO_2 surface, where the position of this modification is shifted to the first pulse. The first laser pulse induces a LIPSS structure, and the second laser interacts with this structure. The scattering of the second laser pulse results most likely in the formation of an SPP which increases the height of the LIPSS structures formed by the first laser beam and irradiated by the second. This increase in height leads to deformation of the overlying SiO_2 layer, resulting in periodic deformation of the SiO_2 surface. A similar explanation can be used for the overlap of 3 or 4 points where further increase in LIPSS height can result in cracking of the overlying SiO_2 layer, see Figure 8. Furthermore, in the 3-point and, 4-point geometry a delamination and cracking of the SiO_2 layer especially nearby the first pulse can be detected. The first laser pulse induces a modification of the

silicon, like amorphization, as well as a partial delamination of the SiO_2 layer, which manifests as a local bulge. It can be assumed that subsequent pulses overlapping these pre-modified regions result in increased absorption due to the altered material state. This enhanced absorption as well as the renewed mechanical stressing of the already delaminated areas through laser-induced thermal stress and shock waves promotes the disintegration of the SiO_2 layer, which is evident through a distinct local increase in surface roughness. This mechanism explains why delamination and cracking of the SiO_2 layer predominantly occur at the positions of earlier pulses.

5. Conclusion

Irradiation of SiO_2/Si(100) systems with a single, Gaussian-profile infrared femtosecond laser pulse (λ = 1030 nm, Δt_p = 260 fs) produces two distinct phenomena:

- A central bulge, created by localized partial vaporization of Si beneath the SiO_2 confinement layer.
- Sub-surface LIPSS forming in a ring around the bulge, characterized by Type LSFL-I periodicity (~1 µm) and oriented perpendicular to the laser polarization.

The sub-surface modification need a laser fluence about 233 – 237 mJ/cm². The formation of LIPSS is associated with the recrystallization and amorphization of the silicon near the surface. This effect is caused by the laser-induced melting of the material and its subsequent re-solidification. One possible cause of LIPSS formation is the propagation of an SPP due to the laser-induced increase in the free carrier density, whereby the process is supported by the SiO_2 confinement. At the current state, however, the influence of interference effects cannot be ruled out. In addition to the single pulse analysis, the overlap of the pulses shows that a pre-modification (amorphization and especially recrystallization) can influence the LIPSS formation. The area of the LIPSS region of two separated single pulses is larger than that of two overlapping pulses at distances below 15 µm. this effect is particularly pronounced parallel to the polarization or perpendicular to the LIPSS. In the next step, comprehensive studies on the thickness, refractive index, and defect density of SiO_2 layers will allow to disentangle the respective roles of surface plasmon polaritons (SPPs) and optical interference effects. Utilizing ultrafast pump–probe imaging, it becomes possible to directly observe SPP excitation and monitor the dynamics of energy deposition as they unfold in real time. Additionally, by investigating the impact of sequential laser pulses, by varying the geometric sequence of the different pulses, the evolution of existing laser-induced periodic surface structures (LIPSS) can be explored. In addition, the use of fs-lasers with shorter wavelengths is being investigated to further clarify the cause of LIPSS formation. Together, these insights demonstrate how careful manipulation of femto-second laser parameters and thin-film confinement can be harnessed to pattern buried interfaces and surface topographies with sub-micrometer precision and to increase the understanding of the LIPSS formation.

Acknowledgments

The authors thanks Toni Liebeskind for the chemical cleaning and etching of the Si substrates, Ivonne Mauersberger for the AFM measurements and Agnes Mill for the lamella preparation by FIB.

References

[1] O. Varlamova, J. Reif, M. Stolz, R. Borcia, I.D. Borcia, and M. Bestehorn: Eur. Phys. J. B., 92, (2019) 91.
[2] H. Vaghasiya and P.-T. Miclea: Opt., 4, (2023) 538.
[3] W. Liu, L. Jiang, W. Han, J. Hu, X. Li, J. Huang, S. Zhan, and Y. Lu: Opt. Express, 27, (2019) 9782.
[4] S. Kawabata, S. Bai, K. Obata, G. Miyaji, and K. Sugioka: Int. J. Extreme Manuf., 5, (2023) 015004.
[5] Y.-F. Gao, C.-Y. Yu, B. Han, M. Ehrhardt, P. Lorenz, L.-F. Xu, and R.-H. Zhu: Surf. Interfaces, 19, (2020) 100538.
[6] J. Bonse, S. Baudach, J. Krüger, W. Kautek, and M. Lenzner: Appl. Phys. A, 74, (2002) 19.
[7] Y. Borodaenko, S. Syubaev, S. Gurbatov, A. Zhizhchenko, A. Porfirev, S. Khonina, E. Mitsai, A.V. Gerasimenko, A. Shevlyagin, E. Modin, S. Juodkazis, E.L. Gurevich, and A.A. Kuchmizhak: ACS Appl. Mater. Interfaces, 13, (2021) 54551.
[8] J. Sládek, Y. Levy, T.J.Y. Derrien, Z. Bryknar, and N.M. Bulgakova: Appl. Surf. Sci., 605, (2022) 154664.
[9] J. Bonse, S. Hoehm, S.V. Kirner, A. Rosenfeld, and J. Krueger: IEEE J. Sel. Top. Quantum Electron., 23, (2017) 9000615.
[10] M. Birnbaum: J. Appl. Phys., 36, (1965) 3688.
[11] J. Bonse, S.V. Kirner, and J. Krüger: Laser-induced periodic surface structures (LIPSS), Handbook of laser micro-and nano-engineering, ed. by K. Sugioka, (Springer, Cham, 2020) p. 879.
[12] J. Bonse and S. Gräf: Laser Photonics Rev., 14, (2020) 2000215.
[13] J.F. Young, J.S. Preston, H.M. van Driel, and J.E. Sipe: Phys. Rev. B, 27, (1983) 1155.
[14] J. Sipe, J.F. Young, J. Preston, and H. Van Driel: Phys. Rev. B, 27, (1983) 1141.
[15] Y. Liu, Y. Ding, J. Xie, L. Xu, I.W. Jeong, and L. Yang: Mater Design, 225, (2023) 111443.
[16] I. Gnilitskyi, V. Gruzdev, N.M. Bulgakova, T. Mocek, and L. Orazi: Appl. Phys. Lett., 109, (2016) 143101.
[17] P. Nürnberger, H.M. Reinhardt, H.-C. Kim, E. Pfeifer, M. Kroll, S. Müller, F. Yang, and N.A. Hampp: Appl. Surf. Sci., 425, (2017) 682.
[18] C. Florian, J.-L. Déziel, S.V. Kirner, J. Siegel, and J. Bonse: Nanomaterials, 10, (2020) 147.
[19] Y. Liao, J.Y. Degorce, and M. Meunier, Appl. Phys. A, 82, (2006) 679.
[20] M. Ehrhardt, B. Han, F. Frost, P. Lorenz, and K. Zimmer: Appl. Surf. Sci., 470, (2019) 56.
[21] J. Bonse; S. Höhm; S.V. Kirner, A. Rosenfeld, and J. Krüger: IEEE J. Sel. Top. Quantum Electron., 23, (2016) 9000615 .
[22] S. Gräf: Adv. Opt. Technol., 9, (2020) 11.
[23] A. San-Blas; M. Martinez-Calderon; E. Granados; M. Gómez-Aranzadi; A. Rodríguez, and S.M. Olaizola: Surf. Interfaces.: 25, (2021) 101205.

[24] P. Hauschwitz, J. Martan, R. Bičišťová, C. Beltrami, D. Moskal, A. Brodsky, N. Kaplan, J. Mužík, D. Štepánková, and J. Brajer: Sci Rep, 11, (2021), 22944.
[25] J.M. Liu: Opt. Lett., 7, (1982) 196.
[26] D. Franta, P. Franta, J. Vohánka, M. Čermák, and I. Ohlídal: J. Appl. Phys., 123, (2018) 185707.
[27] P. Nürnberger: Laser-induzierte Selbstorganisation an äußeren und inneren Grenzflächen, (2017), Philipps-Universität Marburg, https://doi.org/10.17192/z2017.0516.
[28 J.Y.D. Thibault, K. Jörg, and B. Jörn: J. Opt.: 18, (2016) 115007.
[29] S. Anisimov, B. Kapeliovich, and T. Perelman: Zh. Eksp. Teor. Fiz, 66, (1974) 375.
[30] E.G. Gamaly and A. Rode: JOSA B, 31, (2014) C36.
[31] L. Rapp, B. Haberl, J.E. Bradby, E.G. Gamaly, J.S. Williams, and A.V. Rode: Appl. Phys. A, 114, (2014) 33.

(Received: April 16, 2025, Accepted: August 31, 2025)